We are IntechOpen, the world's leading publisher of Open Access books Built by scientists, for scientists

6,900
Open access books available

185,000
International authors and editors

200M
Downloads

Our authors are among the

154
Countries delivered to

TOP 1%
most cited scientists

12.2%
Contributors from top 500 universities



WEB OF SCIENCE™

Selection of our books indexed in the Book Citation Index in Web of Science™ Core Collection (BKCI)

Interested in publishing with us?
Contact book.department@intechopen.com

Numbers displayed above are based on latest data collected.
For more information visit www.intechopen.com



Chapter 6

Edge Detection in Biomedical Images Using Self-Organizing Maps

Lucie Gráfová, Jan Mareš, Aleš Procházka and Pavel Konopásek

Additional information is available at the end of the chapter

http://dx.doi.org/10.5772/51468

1. Introduction

The application of self-organizing maps (SOMs) to the edge detection in biomedical images is discussed. The SOM algorithm has been implemented in MATLAB program suite with various optional parameters enabling the adjustment of the model according to the user's requirements. For easier application of SOM the graphical user interface has been developed. The edge detection procedure is a critical step in the analysis of biomedical images, enabling for instance the detection of the abnormal structure or the recognition of different types of tissue. The self-organizing map provides a quick and easy approach for edge detection tasks with satisfying quality of outputs, which has been verified using the high-resolution computed tomography images capturing the expressions of the Granulomatosis with polyangiitis. The obtained results have been discussed with an expert as well.

2. Self-organizing map

2.1. Self-organizing map in edge detection performance

The self-organizing map (SOM) [5, 9] is widely applied approach for clustering and pattern recognition that can be used in many stages of the image processing, e. g. in color image segmentation [18], generation of a global ordering of spectral vectors [26], image compression [25], binarisation document [4] etc.

The edge detection approaches based on SOMs are not extensively used. Nevertheless there are some examples of SOM utilization in edge detection, e. g. texture edge detection [27], edge detection by contours [13] or edge detection performed in combination with conventional edge detector [24] and methods of image de-noising [8] .

In our case, the SOM has been utilized in edge detection process in order to reduce the image intensity levels.

INTECH
open science | open minds

© 2013 Gráfová et al.; licensee InTech. This is an open access article distributed under the terms of the Creative Commons Attribution License (http://creativecommons.org/licenses/by/3.0), which permits unrestricted use, distribution, and reproduction in any medium, provided the original work is properly cited.

2.2. Structure of self-organizing map

A SOM has two layers of neurons, see Figure 1.

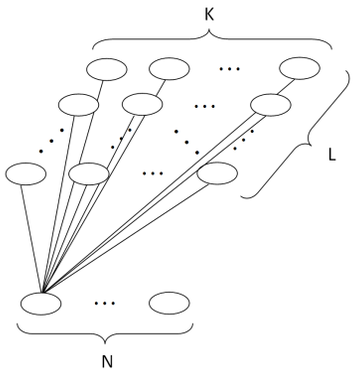


Figure 1. Structure of SOM

The input layer (size Nx1) represents input data $\mathbf{x_1}$, $\mathbf{x_2}$, ..., $\mathbf{x_M}$ (M inputs, each input is N dimensional). The output layer (size KxL), that may have a linear or 2D arrangement, represents clusters in which the input data will be grouped. Each neuron of the input layer is connected with all neurons of the output layer through the weights $\mathbf{W}$ (size of the weight matrix is KxLxN).

2.3. Training of self-organizing map

A SOM is neural network with *unsupervised* type of learning, i. e. no cluster values denoting an a priori grouping of the data instances are provided.

The learning process is divided in *epochs*, during which the entire batch of input vectors is processed. The epoch involves the following steps:

1. Consecutive submission of an input data vector to the network.
2. Calculation of a distances between the input vector and the weight vectors of the neurons of the output layer.
3. Selection of the nearest (the most similar) neuron of the output layer to the presented input data vector.
4. An adjustment of the weights.

SOM can be trained in either *recursive* or *batch mode*. In recursive mode, the weights of the winning neurons are updated after each submission of an input vector, whereas in batch mode, the weight adjustment for each neuron is made after the entire batch of inputs has been processed, i. e. at the end of an epoch.

The weights adapt during the learning process based on a competition, i. e. the nearest (the most similar) neuron of the output layer to the submitted input vector becomes a winner and its weight vector and the weight vectors of its neighbouring neurons are adjusted according to

$$\mathbf{W} = \mathbf{W} + \lambda \, \phi_s \, (\mathbf{x_i} - \mathbf{W}), \tag{1}$$

http://dx.doi.org/10.5772/51468

where $\mathbf{W}$ is the weight matrix, $\mathbf{x_i}$ the submitted input vector, λ the learning parameter determining the strength of the learning and ϕ_s the neighbourhood strength parameter determining how the weight adjustment decays with distance from the winner neuron (it depends on s, the value of the neighbourhood size parameter).

The learning process can be divided into two phases: *ordering* and *convergence*. In the ordering phase, the topological ordering of the weight vectors is established using reduction of learning rate and neighbourhood size with iterations. In the convergence phase, the SOM is fine tuned with the shrunk neighbourhood and constant learning rate. [23]

2.3.1. Learning Parameter

The *learning parameter*, corresponding to the strength of the learning, is usually reduced during the learning process. It decays from the *initial value* to the *final value*, which can be reached already during the learning process, not only at the end of the learning. There are several common forms of the decay function (see Figure 2):

1. No decay

$$\lambda_t = \lambda_0, \tag{2}$$

2. Linear decay

$$\lambda_t = \lambda_0 \left(1 - \frac{t}{\tau}\right), \tag{3}$$

3. Gaussian decay

$$\lambda_t = \lambda_0 \mathrm{e}^{-\frac{t^2}{2\tau^2}}, \tag{4}$$

4. Exponential decay

$$\lambda_t = \lambda_0 \mathrm{e}^{-\frac{t}{\tau}}, \tag{5}$$

where T is the total number of iterations, λ_0 and λ_t are the initial learning rate and that at iteration t, respectively. The learning parameter should be in the interval $\langle 0.01,\ 1 \rangle$.

2.3.2. Neighbourhood

In the learning process not only the *winner* but also the *neighbouring* neurons of the winner neuron learn, i. e. adjust their weights. All neighbour weight vectors are shifted towards the submitted input vector, however, the winning neuron update is the most pronounced and the farther away the neighbouring neuron is, the less its weight is updated. This procedure of the weight adjustment produces *topology preservation*.

There are several ways how to define a neighbourhood (some of them are depicted in Figure 3).

The initial value of the *neighbourhood size* can be up to the size of the output layer, the final value of the neighbourhood size must not be less than 1. The *neighbourhood strength parameter*,

determining how the weight adjustment of the neighbouring neurons decays with distance from the winner, is usually reduced during the learning process (as well as the learning parameter, analogue of Equations 2–5 and Figure 2). It decays from the *initial value* to the *final value*, which can be reached already during the learning process, not only at the end of the learning process. The neighbourhood strength parameter should be in the interval $\langle 0.01,\ 1\rangle$. The Figure 4 depicts one of the possible development of neighbourhood size and strength parameters during the learning process.

2.3.3. Weights

The resulting weight vectors of the neurons of the output layer, obtained at the end of the learning process, represent the centers of the clusters. The resulting patterns of the weight vectors may depend on the type of the *weights initialization*. There are several ways how to initialize the weight vector, some of them are depicted in Figure 5.

2.3.4. Distance Measures

The criterion for victory in the competition of the neurons of the output layer, i. e. the measure of the distance between the presented input vector and its weight vectors, may have many forms. The most commonly used are:

1. Euclidean distance

$$d_j = \sqrt{\sum_{i=1}^{N} \left(x_i - w_{ji}\right)^2}, \tag{6}$$

2. Correlation

$$d_j = \sum_{i=1}^{N} \frac{(x_i - \overline{x})(w_{ji} - \overline{w_j})}{\sigma_x \sigma_{w_j}}, \tag{7}$$

3. Direction cosine

$$d_j = \frac{\sum_{i=1}^{N} x_i w_{ji}}{\|x_i\| \|w_{ji}\|}, \tag{8}$$

4. Block distance

$$d_j = \sum_{i=1}^{N} |x_i - w_{ji}|, \tag{9}$$

where x_i is i-th component of the input vector, w_{ji} i-th component of the j-th weight vector, N dimension of the input and weight vectors, $\overline{x}$ mean value of the input vector x, $\overline{w_j}$ mean value of the weight vector w_j, σ_x standard deviation of the input vector x, σ_{w_j} standard deviation of the weight vector w_j, $\|x_i\|$ length of the input vector x and $\|w_{ji}\|$ length of the weight vector w_j.

http://dx.doi.org/10.5772/51468

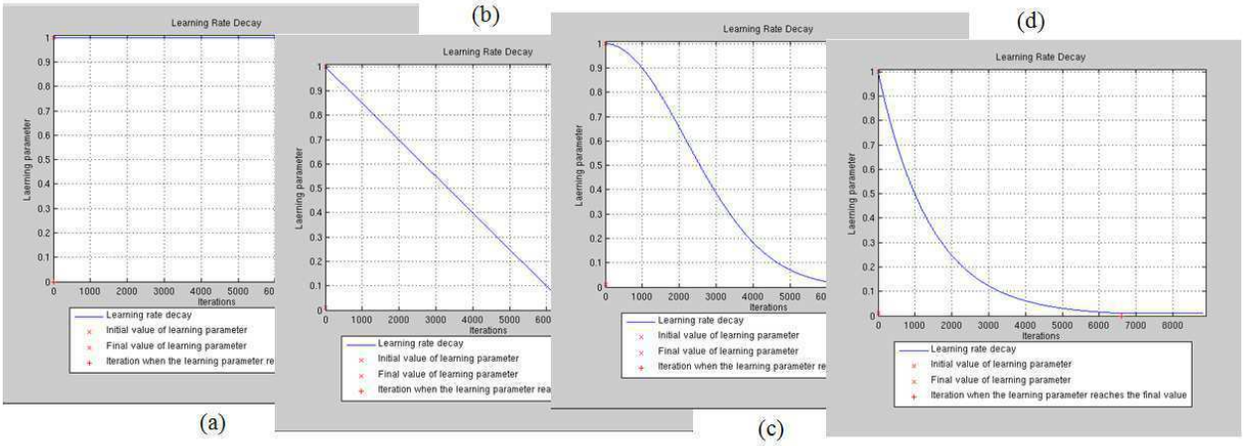


Figure 2. Learning rate decay function (dependence of the value of the learning parameter on the number of iterations): (a) No decay, (b) Linear decay, (c) Gaussian decay, (d) Exponential decay

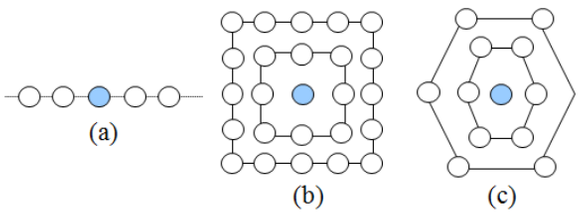


Figure 3. Types of neighbourhood: (a) Linear arrangements, (b) Square arrangements, (c) Hexagonal arrangements

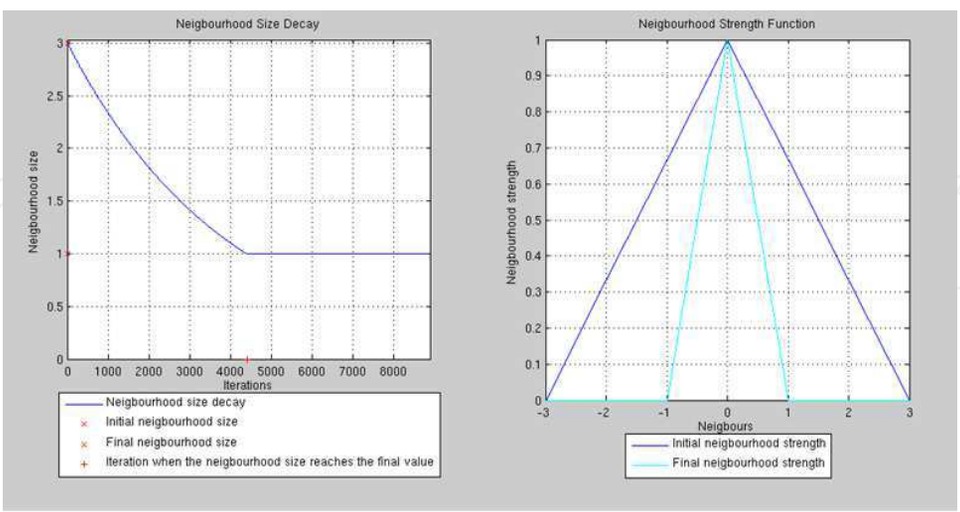


Figure 4. Neighbourhood size decay function (dependence of the neighbourhood size on the number of iterations) and neighbourhood strength decay function (dependence of the value of the neighbourhood strength on the distance from the winner)

2.3.5. Learning Progress Criterion

The *learning progress criterion*, minimized over the learning process, is the sum of distances between all input vectors and their respective winning neuron weights, calculated after the end of each epoch, according to

$$D = \sum_{i=1}^{k} \sum_{n \in c_i} (\mathbf{x_n} - \mathbf{w_i})^2, \tag{10}$$

where $\mathbf{x_n}$ is the n-th input vector belonging to cluster c_i whose center is represented by $\mathbf{w_i}$ (e. i. the weight vector of the winning neuron representing cluster c_i).

The weight adjustment corresponding to the smallest learning progress criterion is the result of the SOM learning process, see Figure 6. These weights represent the cluster centers.

For the best result, the SOM should be run several times with various settings of SOM parameters to avoid detection of local minima and to find the global optimum on the error surface plot.

2.3.6. Errors

The errors of trained SOM can be evaluated according to

1. Learning progress criterion (see Equation 10),
2. Normalized learning progress criterion

$$E = \frac{1}{M} \sum_{i=1}^{k} \sum_{n \in c_i} (\mathbf{x_n} - \mathbf{w_i})^2, \tag{11}$$

3. Normalized error in the cluster

$$E = \frac{1}{k} \sum_{i=1}^{k} \frac{1}{M_i} \sum_{n \in c_i} (\mathbf{x_n} - \mathbf{w_i})^2, \tag{12}$$

4. Error in the i-th cluster

$$E_i = \sum_{n \in c_i} (\mathbf{x_n} - \mathbf{w_i})^2, \tag{13}$$

5. Normalized error in the i-th cluster

$$E_i = \frac{1}{M_i} \sum_{n \in c_i} (\mathbf{x_n} - \mathbf{w_i})^2, \tag{14}$$

where $\mathbf{x_n}$ is the n-th input vector belonging to cluster c_i whose center is represented by w_i (e. i. the weight vector of the winning neuron representing cluster c_i), M is number of input vectors, M_i is number of input vectors belonging to i-th cluster and k is number of clusters.

For more information about the trained SOM, the distribution of the input vectors in the clusters and the errors of the clusters can be visualized, see Figure 7.

2.3.7. Forming Clusters

The *U-matrix* (the matrix of average distance between weights vectors of neighbouring neurons) can be used for finding of realistic and distinct clusters. The other approach for forming clusters on the map can be to utilize any established clustering method (e. g. K-means clustering). [23, 28]

2.3.8. Validation of Trained Self-organizing Map

The validation of the trained SOM can be done so, a portion of the input data is used for map training and another portion for validation (e. g. in proportion 70:30). Different approach for SOM validation is *n*-fold cross validation with the leave-one out method. [16, 23]

2.4. Using of trained self-organizing map

A trained SOM can be used according the following steps for clustering:

1. Consecutive submission of an input data vector to the network.
2. Calculation of a distances between the input vector and the weight vectors of the neurons of the output layer.
3. Selection of the nearest (the most similar) neuron of the output layer (e. i. the cluster) to the presented input data vector.

2.5. Implementation of self-organizing map

The SOM algorithm has been implemented in MATLAB program suite [17] with various optional parameters enabling the adjustment of the model according to the user's requirements. For easier application of SOM the graphical user interface has been developed facilitating above all the setting of the neural network, see Figure 8.

3. Edge detection

Edge detection techniques are commonly used in image processing, above all for feature detection, feature extraction and segmentation.

The aim of the edge detection process is to detect the object boundaries based on the abrupt changes in the image tones, i. e. to detect discontinuities in either the image intensity or the derivatives of the image intensity.

3.1. Conventional edge detector

The image edge is a property attached to a single pixel. However it is calculated from the image intensity function of the adjacent pixels.

Many commonly used edge detection methods (*Roberts* [22], *Prewitt* [20], *Sobel* [19], *Canny* [6], *Marr-Hildreth* [15] etc), employ derivatives (the first or the second one) to measure the rate of change in the'image intensity function. The large value of the first derivative and zero-crossings in the second derivative of the image intensity represent necessary condition for the location of the edge. The differential operations are usually approximated discretely

by proper convolution mask. Moreover, for simplification of derivative calculation, the edges are usually detected only in two or four directions.

The essential step in edge detection process is *thresholding*, i. e. determination of the threshold limit corresponding to a dividing value for the evaluation of the edge detector response either as the edge or non-edge. Due to the thresholding, the result image of the edge detection process is comprised only of the edge (white) and non-edge (black) pixels. The quality of thresholding setting has an impact on the quality of the whole edge detection process, i. e. exceedingly small value of the threshold leads to assignment of the noise as the edge, on the other hand exceedingly large value of the threshold leads to omission of some significant edges.

3.2. Self-organizing map

A SOM may facilitate the edge detection task, for instance by reducing the dimensionality of an input data or by segmentation of an input data.

In our case, the SOM has been utilized for the reduction of image intensity levels, from 256 to 2 levels. Each image has been transformed to mask (3x3), see Table 1, that forms the set of input vectors (9-dimensional). The input vectors have been then classified into 2 classes according to the weights of the beforehand trained SOM. The output set of the classified vectors has been reversely transformed into the binary (black and white) image.

Due to this image preprocessing using SOM, the following edge detection process has been strongly simplified, i. e. only the *numerical gradient* has been calculated

$$G = \sqrt{G_x^2 + G_y^2}, \tag{15}$$

where G is the edge gradient, G_x and G_y are values of the first derivative in the horizontal and in the vertical direction, respectively.

The ability of SOM for edge detection in biomedical images has been tested using the high-resolution computed tomography (CT) images capturing the expressions of the Granulomatosis with polyangiitis disease.

4. Granulomatosis with polyangiitis

4.1. Diagnosis of granulomatosis with polyangiitis

Granulomatosis with polyangiitis (GPA), in the past also known as Wegener's granulomatosis is a disease belonging to the group of vasculitic diseases affecting mainly small caliber blood vessels [7].

They can be distinguished from other vasculitides by the presence of *ANCA* antibodies (ANCA - Anti- Neutrophil Cytoplasmic Antibodies). GPA is quite a rare disease, its yearly incidence is around 10 cases per million inhabitants. The course of the disease is extremely variable on the one hand there are cases of organ limited disease that affects only single organ, on the other hand there is a possibility of generalized disease affecting multiple organs and threatening the patients life. Diagnostics of this disease has been improved

http://dx.doi.org/10.5772/51468

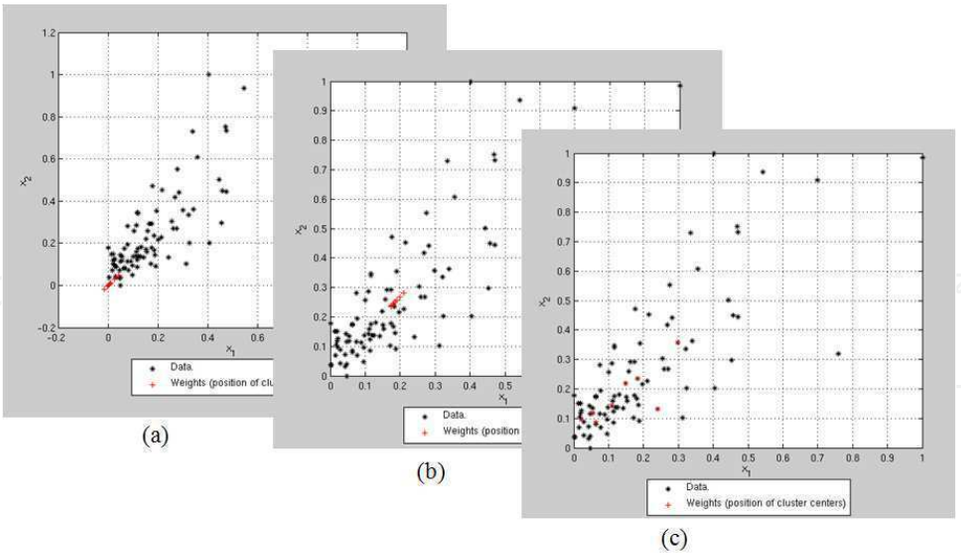


Figure 5. Weight vectors initialization: (a) Random small numbers, (b) Vectors near the center of mass of inputs, (c) Some of the input vectors are randomly chosen as the'initial weight vectors

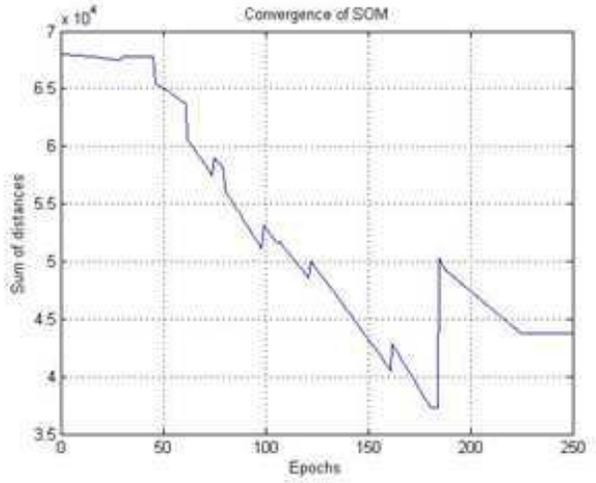
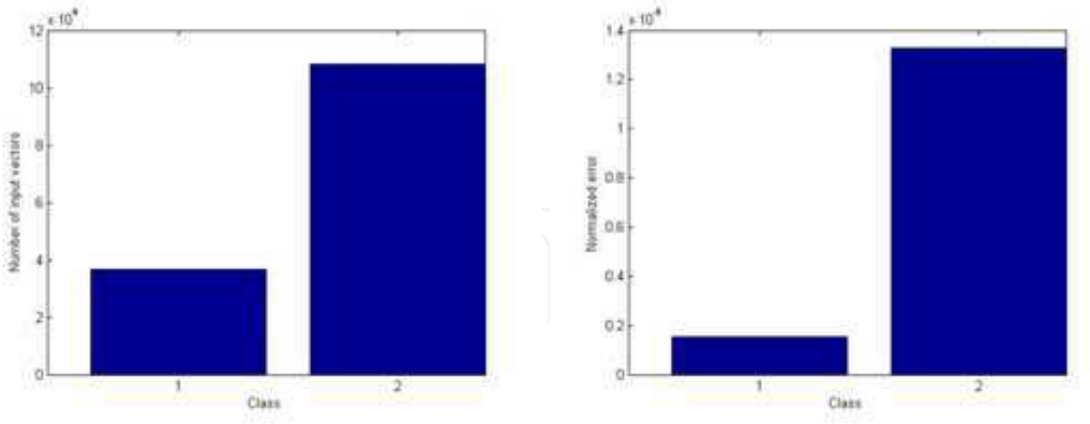


Figure 6. The training criterion of the learning process.
The figure shows the example of the evolution of the training criterion (sum of the distances between all input vectors and their respective winning neuron weights) as the function of the number of epochs. In this case, the smallest sum of distances was achieved in the 189th epoch

P1	P2	P3
P4	P5	P6
P7	P8	P9

Table 1. The image mask used for the preparation of the set of the input vectors.
The mask (9 adjacent pixels) was moved over the whole image pixel by pixel row-wise and the process continued until the whole image was scanned. From each location of the scanning mask in the image the single input vector has been formed, i. e. $\mathbf{x} = (P1, P2, P3, P4, P5, P6, P7, P8, P9)$, where $P1$–$P9$ denote the intensity values of the image pixel. The (binary) output value of SOM for each input vector replaced the intensity value in the position of the pixel with original intensity value $P5$



(a) (b)

Figure 7. The additional information about the SOM result.
(a) The distribution of the input vectors in the clusters, (b) The errors of the clusters (the mean value of the distance between the respective input vectors and the cluster center with respect to the maximum value of the distance)

by the discovery of ANCA antibodies and their routine investigation since the nineties of the past century. The onset of GPA may occur at any age, although patients typically present at age 35–55 years [11].

A classic form of GPA is characterized by necrotizing granulomatous vasculitis of the upper and lower respiratory tract, glomerulonefritis, and small-vessel vasculitis of variable degree. Because of the respiratory tract involvement nearly all the patients have some respiratory symptoms including cough, dyspnea or hemoptysis. Due to this, nearly all of them have a chest X-ray at the admission to the hospital, usually followed by a high-resolution computed CT scan. The major value of CT scanning is in the further characterization of lesions found on chest radiography.

The spectrum of high-resolution CT findings of GPA is broad, ranging from nodules and masses to ground glass opacity and lung consolidation. All of the findings may mimic other conditions such as pneumonia, neoplasm, and noninfectious inflammatory diseases [2].

The prognosis of GPA depends on the activity of the disease and disease-caused damage and response to therapy. There are several drugs used to induce remission, including cyclophosphamide, glucocorticoids or monoclonal anti CD 20 antibody rituximab. Once the remission is induced, mainly azathioprin or mycophenolate mofetil are used for its maintenance.

Unfortunately, relapses are common in GPA. Typically, up to half of patients experience relapse within 5 years [21].

4.2. Analysis of granulomatosis with polyangiitis

Up to now, all analysis of CT images with GPA expressions have been done using manual measurements and subsequent statistical evaluation [1, 3, 10, 12, 14]. It has been based on the experience of a radiologist who can find abnormalities in the CT scan and who is able to

classify types of the finding. The standard software [1] used for CT image visualization usually includes some interactive tools (zoom, rotation, distance or angle measurements, etc.) but no analysis is done (e. g. detection of the abnormal structure or recognition of different types of tissue). Moreover, there is no software customized specifically for requirements of GPA analysis.

Therefore, there is a place to introduce a new approach for analysis based on SOM. CT finding analysis is then less time consuming and more precise.

5. Results and discussion

The aim of the work has been to detect all three expression forms of the GPA disease in high-resolution CT images (provided by Department of Nephrology, First Faculty of Medicine and General Faculty Hospital, Prague, Czech Republic) using the SOM, i. e. to detect *granulomatosin*, *mass* and *ground-glass*, see Figure 10a, 11a, 12a. The particular expression forms occur often together, therefore there has been the requirement to distinguish the particular expression forms from each other.

Firstly, the SOM has been trained using the test image, see Figure 9 (For detailed information about the training process, please see Table 2).

Secondly, the edge detection of the validating images has been done using the result weights from the SOM training process, see Figure 10b, 11b, 12b (For detailed information about the edge detection process, please see Table 3).

Setting description	**Value**
Size of the output layer	(1,2)
Type of the weights initialization	Some of the input vectors are randomly chosen as the initial weight vectors.
Initial value of the'learning parameter	1
Final value of the learning parameter	0.1
A point in the learning process in which the learning parameter reaches the final value	0.9
Initial value of the cneighbourhood size parameter	2
Final value of the cneighbourhood size parameter	1
A point in the learning process in which the neighbourhood size parameter reaches the final value	0.75
Type of the distance measure	1
Type of the learning rate decay function	Exponential
Type of neighbourhood size strength function	Linear
Type of the neighbourhood size rate decay function	Exponential
Number of the epochs	500

Table 2. Setting of the SOM training process

[1] Syngo Imaging XS-VA60B, Siemens AG Medical Solutions, Health Services, 91052 Erlangen, Germany

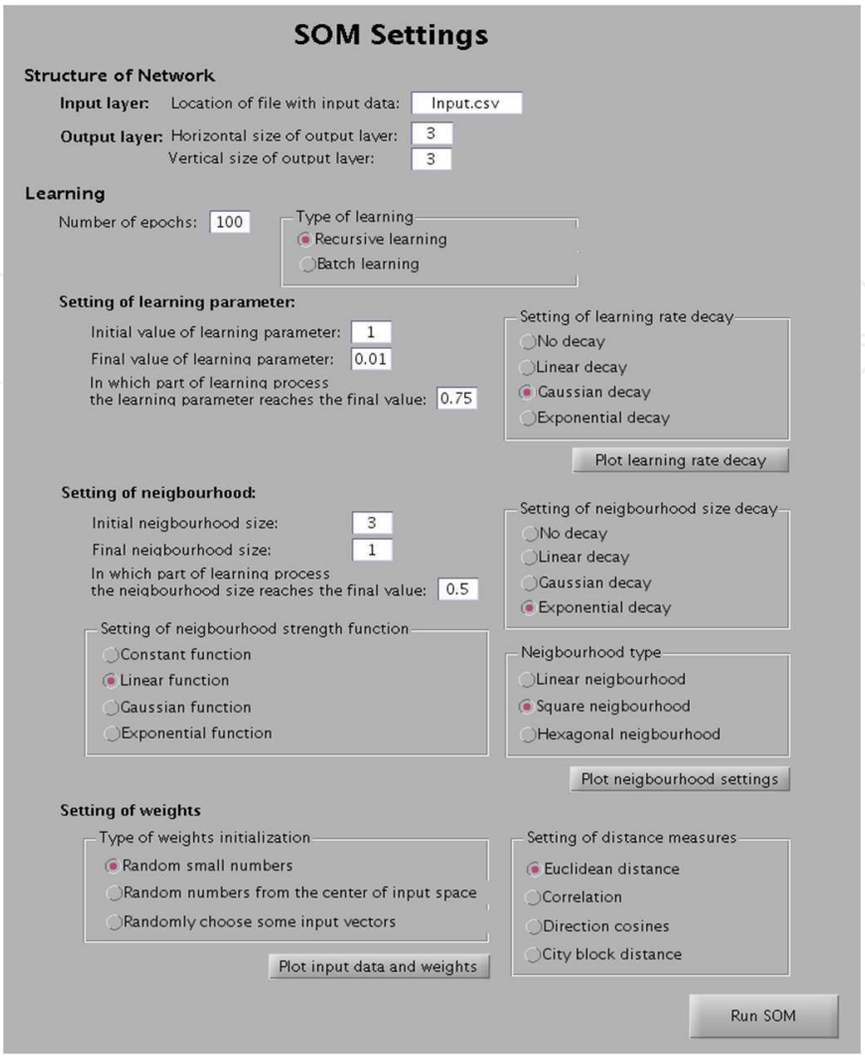


Figure 8. The graphical user interface of the software using SOM for clustering

Stages	Description
Image preprocessing	Histogram matching of the input image to the test image.
Image transformation	The image is transformed to M masks (3x3) that form the set of *M* input vectors (9 dimensional).
Clustering using SOM	The set of the input vectors is classified into 2 classes according to the obtained weights from the SOM training process.
Reverse image transformation	The set of classified input vectors is reversely transformed into the image. The intensity values are replaced by the values of the class membership.
Edge detection	Computation of image gradient.

Table 3. Stages of the edge detection process

http://dx.doi.org/10.5772/51468

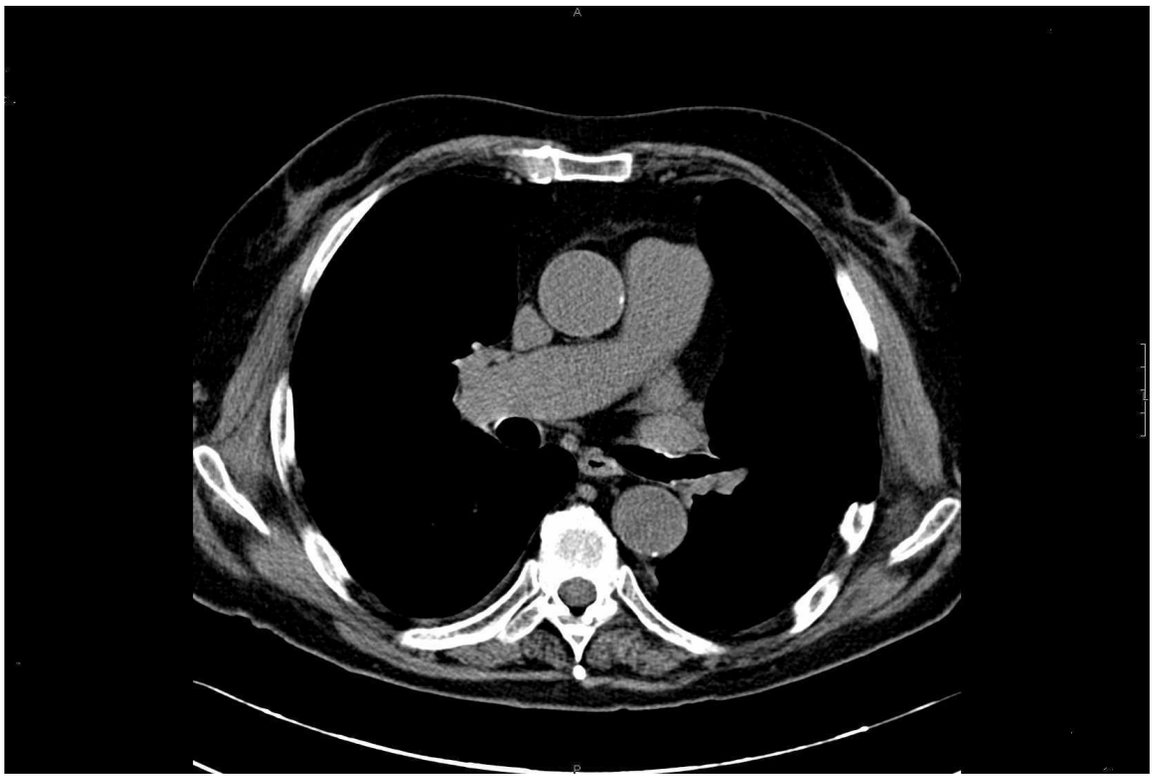


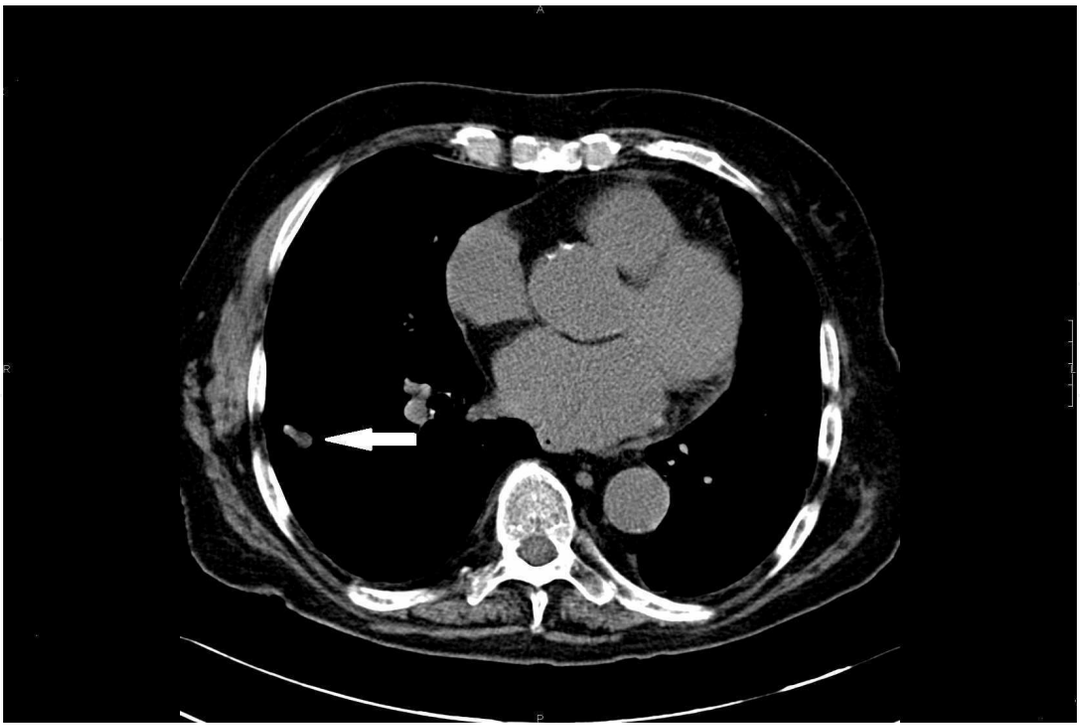
Figure 9. Test image (transverse high-resolution CT image of both lungs)

The obtained results have been discussed with an expert from Department of Nephrology of the First Faculty of Medicine and General Teaching Hospital in Prague.

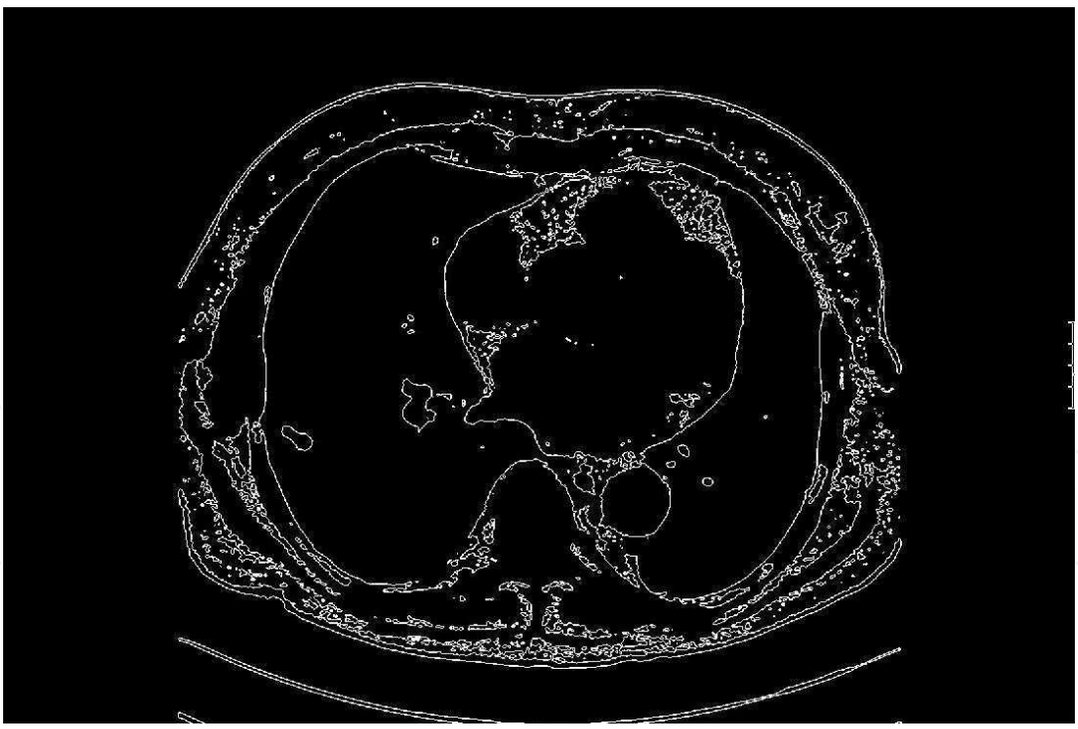
In the first case, a high-resolution CT image capturing a granuloma in the left lung has been processed, see Figure 10a. The expert has been satisfied with the quality of the GPA detection (see Figure 10b) provided by the SOM, since the granuloma has been detected without any artifacts.

In the second case, the expert has pointed out that the high-resolution CT image, capturing both masses and ground-glass (see Figure 11a, 12a), was problematic to be evaluated. The possibility of the detection of the masses was aggravated by the ground-glass surrounding the lower part of the first mass and the upper part of the second mass. The artifacts, which originated in the coughing movements of the patient ('wavy' lower part of the image), made the detection process of the masses and the ground-glass difficult as well. Despite these inconveniences, the expert has confirmed, that the presented software has been able to distinguish between the particular expression forms of GPA with satisfying accuracy and it has detected the mass and ground-glass correctly (see Figure 11b, 12b, 12c).

In conclusion, the presented SOM approach represents a new helpful approach for GPA disease diagnostics.



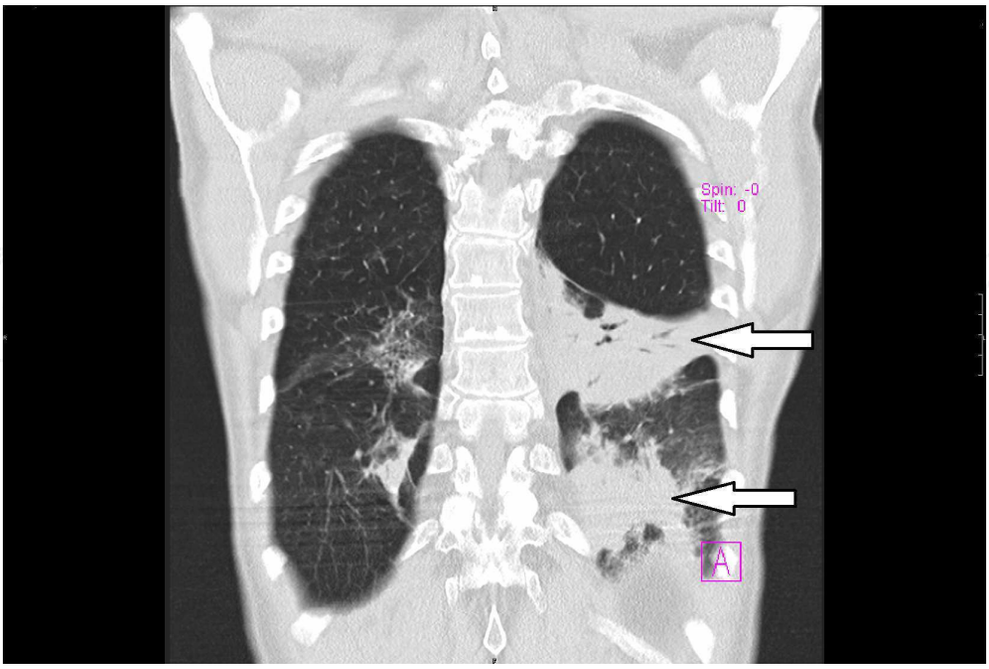
(a)



(b)

Figure 10. Detection of granuloma.
(a) Transverse high-resolution CT image of both lungs with active granulomatosis (white arrow).
b) The edge detection result obtained by the SOM. The granulomatosin is detected with sufficient accuracy

http://dx.doi.org/10.5772/51468

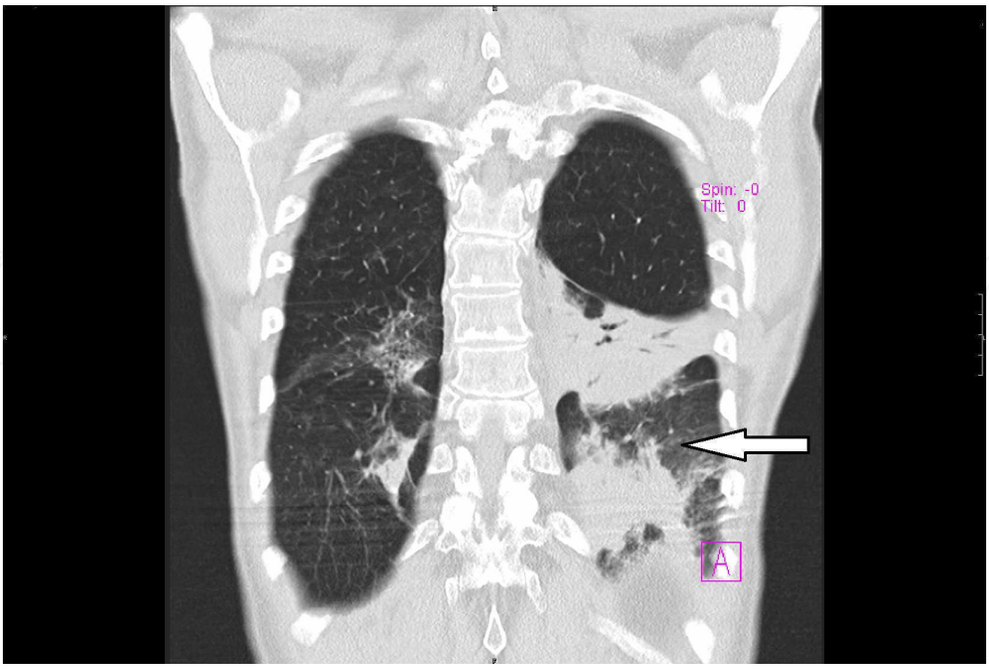


(a)



(b)

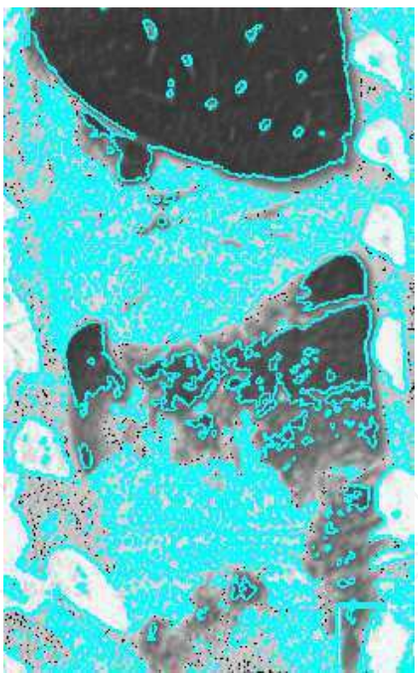
Figure 11. Detection of masses.
(a) Coronal high-resolution CT image of both lungs with masses (white arrows). Possibility of the detection of the masses is aggravated by the'ground-glass surrounding the lower part of the first mass and the upper part of the second mass. The artifacts originated by coughing movements of the patient makes the detection process difficult as well.
(b) The edge detection result obtained by the SOM. The'masses are detected and distinguished from the ground-glass with sufficient accuracy



(a)



(b)



(c)

Figure 12. Detection of ground-glass.
(a) Coronal high-resolution CT image of both lungs with ground-glasses (white arrows). Possibility of the detection of the ground-glasses is complicated by the masses in close proximity to the ground-glasses. The artifacts originated by coughing movements of the patient makes the detection process hard as well.
(b) The edge detection result obtained by the SOM. The ground-glasses are detected and distinguished from the masses.
(c) The overlap of the original CT image and the edge detection result (cyan color)

http://dx.doi.org/10.5772/51468

6. Conclusions

The edge detection procedure is a‘critical step in the analysis of biomedical images, enabling above all the detection of the abnormal structure or the‘recognition of different types of tissue.

The application of SOM for edge detection in biomedical images has been discussed and its contribution to the solution of the edge detection task has been confirmed. The‘ability of SOM has been verified using the‘high-resolution CT images capturing all three forms of the expressions of the GPA disease (granulomatosin, mass, ground-glass). Using SOM, particular expression forms of the GPA disease have been detected and distinguished from each other. The obtained results have been discussed by the expert who has confirmed that the SOM provides a quick and easy approach for edge detection tasks with satisfying quality of output.

Future plans are based on the problem extension to three-dimensional space to enable CT image analysis involving (i) pathological finding 3D visualization and (ii) 3D reconstruction of the whole region (using the whole set of CT images).

Acknowledgements

The work was supported by specific university research MSMT No. 21/2012, the reaserch grant MSM No. 6046137306 and PRVOUK-P25/LF1/2.

Author details

Lucie Gráfová[1], Jan Mareš[1], Aleš Procházka[1] and Pavel Konopásek[2]

[1]Department of Computing and Control Engineering, Institute of Chemical Technology, Prague, Czech Republic
[2]Department of Nephrology, First Faculty of Medicine and General Faculty Hospital, Prague, Czech Republic

7. References

[1] Ananthakrishnan, L., Sharma, N. & Kanne, J. P. [2009]. Wegener?s granulomatosis in the chest: High-resolution ct findings, *Am J Roentgenol* 192(3): 676–82.

[2] Annanthakrishan, L., Sharma, N. & Kanne, J. P. [2009]. Wegener‘s granulomatosis in the chest: High-resolution ct findings, *Am J Roentgenol* 192(3): 676–82.

[3] Attali, P., Begum, R., Romdhane, H. B., Valeyre, D., Guillevin, L. & Brauner, M. W. [1998]. Pulmonary wegener?s granulomatosis: changes at follow-up ct, *European Radiology* 8: 1009–1113.

[4] Badekas, E. & Papamarkos, N. [2007]. Document binarisation using kohonen som, *IET Image Processing* 1: 67–84.

[5] Baez, P. G., Araujo, C. S., Fernandez, V. & Procházka, A. [2011]. *Differential Diagnosis of Dementia Using HUMANN-S Based Ensembles*, Springer, Berlin, Germany, chapter 14, pp. 305–324.

[6] Canny, J. [1986]. A computational approach to edge detection, *IEEE Transactions on Pattern Analysis and Machine Intelligence* PAMI-8(6): 679–698.

[7] Jennette, J. C. [2011]. Nomenclature and classification of vasculitis: lessons learned from granulomatosis with polyangiitis (wegener's granulomatosis), *Clin Exp Immunol* 164: 7–10.

[8] Jerhotová, E., Švihlík, J. & Procházka, A. [2011]. *A. Biomedical Image Volumes Denoising via the Wavelet Transform*, InTech, chapter 14.

[9] Kohonen, T. [1989]. *Self-Organization and Associative Memory*, Springer-Verlag.

[10] Komócsi, A., Reuter, M., Heller, M., Muraközi, H., Gross, W. L. & Schnabel, A. [2003]. Active disease and residual damage in treated wegener?s granulomatosis: an observational study using pulmonary high-resolution computed tomography, *European Radiology* 13: 36–42.

[11] Lane, S. E., Watts, R. & Scott, D. G. I. [2005]. Epidemiology of systemic vasculitis, *Curr Rheumatol Rep* 7: 270–275.

[12] Lee, K. S., Kim, T. S., Fujimoto, K., Moriya, H., Watanabe, H., Tateishi, U., Ashizawa, K., Johkoh, T., Kim, E. A. & Kwon, O. J. [2003]. Thoracic manifestation of wegener?s granulomatosis: Ct findings in 30 patients, *European Radiology* 13: 43–51.

[13] Liu, J.-C. & Pok, G. [1999]. Texture edge detection by feature encoding and predictive model, *Proceedings of the IEEE International Conference on Acoustics, Speech, and Signal Processing*, pp. 1105–1108.

[14] Lohrmann, C., Uhl, M., Schaefer, O., Ghanem, N., Kotter, E. & Langer:, M. [2005]. Serial high-resolution computed tomography imaging in patients with wegener granulomatosis: Differentiation between active inflammatory and chronic fibrotic lesions, *Acta Radiologica* 46: 484–491.

[15] Marr, D. & Hildreth, E. [1980]. Theory of edge detection, *Proc. Roy. Soc. Landon*, Vol. B.207, pp. 187–217.

[16] Mitchell, T. [1997]. *Machine Learning*, McGraw-Hill.

[17] Moore, H. [2007]. *Matlab for Engineers*, Pearson, Prentice Hall.

[18] Moreira, J. & Fontuora, L. D. [1996]. Neural-based color image segmentation and classification, *Anais do* IX SIBGRAPI: 47–54.

[19] Pingle, K. K. [1969]. *Visual perception by computer. Automatic Interpretation and Classification of Images*, Academic Press, New York.

[20] Prewitt, J. M. S. [1970]. *Object enhancement and extraction. Picture Processing and Psychophysics*, Academic Press, New York.

[21] Renaudineau, Y. & Meur, Y. L. [2008]. Renal involvement in wegener's granulomatosis, *Clinic Rev Allerg Immunol* 35: 22–29.

[22] Roberts, L. G. [1963]. *Machine Perception of Three Dimensional Solids*, PhD thesis, Massachusetts Institute of Technology, Electrical Engineering Department.

[23] Samarasinghe, S. [2006]. *Neural Networks for Applied Sciences and Engineering: From Fundamentals to Complex Pattern Recognition*.

[24] Sampaziotis, P. & Papamarko, N. [2005]. Automatic edge detection by combining kohonen som and the canny operator, *Proceedings of the 10th Iberoamerican Congress conference on Progress in Pattern Recognition, Image Analysis and Applications*, pp. 954–965.

[25] Sharma, D. K., Gaur, L. & Okunbor, D. [2007]. Image compression and feature extraction using kohonen's self-organizing map neural network, *Journal of Strategic E-Commerce* 5(No. 0): 25–38.

[26] Toivanen, P. J., Ansamäki, J., Parkkinen, J. P. S. & Mielikäinen, J. [2003]. Edge detection in multispectral images using the self-organizing map, *Pattern Recognition Letters* 24: 2987–2994.

[27] Venkatesh, Y. V., K.Raja, S. & Ramya, N. [2006]. Multiple contour extraction from graylevel images using an artificial neural network, *IEEE Transactions on Image Processing* 15: 892–899.

[28] Wilson, C. L. [2010]. *Mathematical Modeling, Clustering Algorithms and Applications*.

IntechOpen

IntechOpen

IntechOpen